Available online at www.sciencedirect.com
SCIENCE DIRECT
Polymer 47 (2006) 1207–1216
polymer
www.elsevier.com/locate/polymer

# Characterization of crosslinked hollow fiber membranes

David W. Wallace [a], Jason Williams [c], Claudia Staudt-Bickel [b], William J. Koros [c,*]

[a] University of Texas, Austin, TX, USA
[b] University of Heidelberg, Heidelberg, Germany
[c] Georgia Institute of Technology, Atlanta, GA, USA

Received 14 August 2005; received in revised form 11 December 2005; accepted 12 December 2005

**Abstract**

As the applications for polymeric membranes expand, new challenges arise. One of the largest of these challenges is the plasticization caused by strongly swelling penetrants such as carbon dioxide at elevated pressures. A considerable amount of material research has investigated crosslinking of dense film membranes to increase plasticization resistance. This paper extends such materials research to include more practically relevant asymmetric hollow fibers. Crosslinkable polyimide fibers were spun and an ester crosslinking reaction was studied using chemical and spectroscopic techniques to characterize the extent of crosslinking and to relate the effect of the reaction on fiber stability. $CO_2$ permeance and $CO_2/CH_4$ selectivity were studied at a variety of pressures and temperatures over time to yield indications of real-world separation performance.


*Keywords:* Crosslinked polyimide; Asymmetric hollow fiber; Gas separation membrane

## 1. Introduction

One of the challenges for polymeric gas separation membranes is the loss of selectivity caused by plasticization. Previous strategies to develop plasticization resistant polymeric membranes have included heat treatment, blending, reactively formed interpenetrating networks, and crosslinking [1–9]. Crosslinking is an attractive option, since it combines relatively easy implementation within acceptable processing conditions and produces significantly improved plasticization resistance as measured by improved selectivity under demanding feed conditions [8]. However, past work has focused primarily on crosslinking dense film membranes.

The challenges of solid-state crosslinking faced in dense film work are magnified in commercially important asymmetric hollow fibers [10]. The aggressive conditions needed to promote crosslinking must be balanced by the need to preserve the delicate morphology needed for optimum separation performance. Aggressive heat treatments of asymmetric hollow fibers, even below the $T_g$ of the polymer, can cause substructure collapse [11], destruction of the integrity of the skin layer, and overall fiber embrittlement. To be practically useful, these negative aspects must be minimized while still creating a fiber that resists $CO_2$ plasticization. This work shows the challenges inherent in maintaining the balance between preserving physical morphology and establishing chemical durability.

## 2. Experimental

### 2.1. Fiber spinning

All fibers described in this work were spun from a 6FDA-based polyimide containing a 3:2 ratio of DAM:DABA diamines as described elsewhere [12]. The DABA groups were monoesterified with 1,3-propane diol prior to spinning (throughout this work, references to propane diol will be assumed to be 1,3-propane diol). Synthesis and esterification were done at the University of Heidelberg and are also described elsewhere [8]. The molecular weight of the final monoesterified polymer (Fig. 1) was found to be approximately 29,000 ($M_n$) using a GPC with universal calibration.

Fibers were spun on the system described by McKelvey et al. [13]. Dope extrusion rates were between 48 and 60 mL/h, and take-up rates varied between 17 and 50 m/min. This corresponded to stable nominal draw ratios between 4 and 9 (fiber take-up rate over extrusion rate, disregarding die swell). The spinning and quench temperatures were 50 °C and the air gap was varied between 5 and 21 cm. Fibers spun at a nominal

* Corresponding author. Address: School of Chemical Engineering, Georgia Institute of Technology, Atlanta, GA 30332-0100, USA
*E-mail address:* william.koros@chbe.gatech.edu (W.J. Koros).

0032-3861/$ - see front matter © 2005 Elsevier Ltd. All rights reserved.
doi:10.1016/j.polymer.2005.12.079

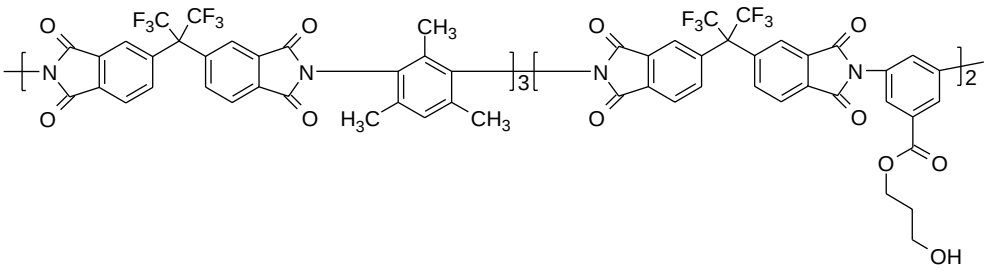

Fig. 1. Simplified structure of 6FDA-DAM:DABA 3:2.

draw ratio of about 9 and an air gap of 5 cm were used for permeation testing. They showed essentially defect-free selectivity (4.2 compared to 4.4 for dense films) for the $O_2/N_2$ separation.

All fibers showed excellent concentricity and were nearly perfectly circular. No macrovoids were evident in optical or SEM microscopy. Fig. 2 shows an SEM image typical of these crosslinkable fibers. Further optimization of the bore fluid to reduce the solvent fraction would be useful to minimize extraction of low molecular weight oligomers into the bore region; however, the membranes are entirely functional in the current forms.

### 2.2. Crosslinking

The crosslinking reaction was driven by heating fibers under vacuum for a set period of time in a preheated vacuum oven. Vacuum was pulled throughout the drying to maximize the driving force for removal of 1,3-propane diol. Not all conditions led to crosslinked fibers, but for convenience, the process of heating will be referred to loosely as either 'heat-treatment' or 'crosslinking' during of this discussion, regardless of whether covalent crosslinks are actually formed. For the primary time–temperature crosslinking experiments, fibers were treated at 200 °C for 6, 12, 24, 48, and 96 h, and for 24 h at 120, 150, 200, 230, and 300 °C.

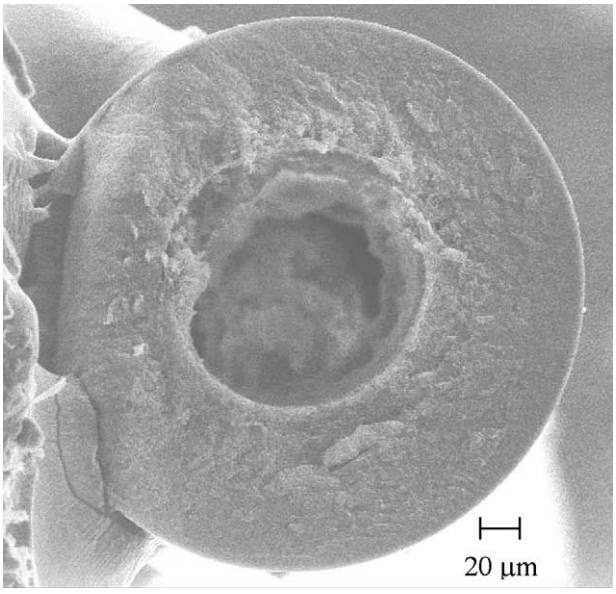


Fig. 2. SEM picture of crosslinkable asymmetric hollow fiber spun from 3:2 polyimide.

### 2.3. Transport

Permeance and selectivity of the fibers were determined using techniques described in detail elsewhere [14]. For mixed gas testing, a model natural gas feed containing 20% $CO_2$ in $CH_4$ was used and a stage cut of less than 1% was maintained to minimize the effects of concentration polarization [15]. Uncertainties in permeance and selectivity were calculated from propagation of error.

### 2.4. TGA-IR

TGA-IR (thermogravimetric analysis-infra-red) was used to analyze the evolution of gases from samples both by weight loss (quantitative) and IR spectroscopy (qualitative). In this work, a Netzsch STA 409 TGA instrument was used with a Bruker Tensor 27 FTIR spectrometer outfitted with a flow-through gas cell and an LN-MCT external detector.

The TGA portion of the instrument was programmed to control temperature, heating rates, and soak times. A flowing nitrogen atmosphere was maintained at all times in the instrument as a carrier gas and to simulate the low vapor pressure of gases evolving during vacuum drying. While this is a valid simulation of the vacuum environment, some differences would likely be expected between the two cases and further study is warranted. IR spectra were continuously monitored and recorded at defined intervals.

## 3. Crosslinking characterization

Three chief methods were used to characterize the crosslinking in hollow fibers, dissolution, TGA-IR, and plasticization resistance. Each method gives complementing data.

### 3.1. Fiber dissolution

The quickest crosslinking crosslinking test is simple dissolution. The polymer used here is fully soluble in tetrahydrofuran (THF) when uncrosslinked, but after crosslinking, the 'infinite' molecular weight makes it insoluble. Fibers subjected to crosslinking at a series of times and temperatures were placed in vials of THF to determine the

Table 1
Observations of swelling and dissolution behavior of fibers in THF

| Crosslinking temperature (°C) | Crosslinking time (h) | | | | |
|---|---|---|---|---|---|
| | 6 | 12 | 24 | 48 | 96 |
| 120 | | | Dissolved | | |
| 150 | | | Nearly dissolved | | |
| 200 | Some swelling | Some swelling | Some swelling | Little swelling | Slight swelling |
| 230 | | | Limited swelling | | |
| 300 | | | No change | | |

existence of crosslinking and the qualitative results are shown in Table 1.

The series of crosslinking temperatures at 24 h time shows a trend in solubility. At 120 °C, the fibers are completely soluble, while at 300 °C, there is no change. The fibers crosslinked at 150 °C largely dissolved; however, some very small, highly swollen pieces were apparent. This behavior indicates some crosslinks have begun to form, but crosslinking has not proceeded sufficiently to stabilize the fibers overall. GPC measurement of the molecular weights of 120 and 150 °C crosslinked fibers support this, showing essentially no change from the raw polymer for the 120 °C fibers, while the 150 °C fibers showed a molecular weight increase of nearly 35% over the original polymer. The trend continues with the fibers crosslinked at 200 and 230 °C which exhibit successively smaller amounts of swelling indicating an increase in crosslinking.

The time series shows a different trend. Fibers were visibly intact in each vial and there is limited difference in solvent stability when fibers are crosslinked at 200 °C between 6 and 96 h. While transport properties are affected by time and temperature of treatment (discussed below), solvent resistance seems to be a function primarily of temperature, a hypothesis that is further supported by the TGA-IR data.

### 3.2. TGA-IR analysis

TGA-IR (thermogravimetric analysis-infrared spectroscopy) studies provide additional insight into the crosslinking process. The quantities and identities of evolved gases can be determined and in principle, the evolution of propane diol could be used to indicate a degree of crosslinking. Unfortunately, the analysis of propane diol was confounded by a significant evolution of *N*-methyl-2-pyrrolidinone (NMP) at the same time.

NMP is used as both a synthesis and spinning solvent and is difficult to wash out, subsequently evolving at the same time as propane diol during heating. Fig. 3 shows the TGA curve for the polymer as it is heated from 20 to 300 °C at 5 °C/min. The curve plots temperature and percent weight loss vs. time.

Two regions of major weight loss are seen, at about 5 and 30 min. The IR data at the first point shows the evolution of absorbed water. Fig. 4 shows the IR spectrum of the gases evolved during the entirety of the second weight loss, as well as spectra for pure propane diol and pure NMP obtained from the NIST Webbook [16].

The spectrum shows that the evolved gas contains both NMP and propane diol. The sample spectrum appears to be a simple addition of the two pure-component spectra, showing both molecules evolving simultaneously (indicated by the

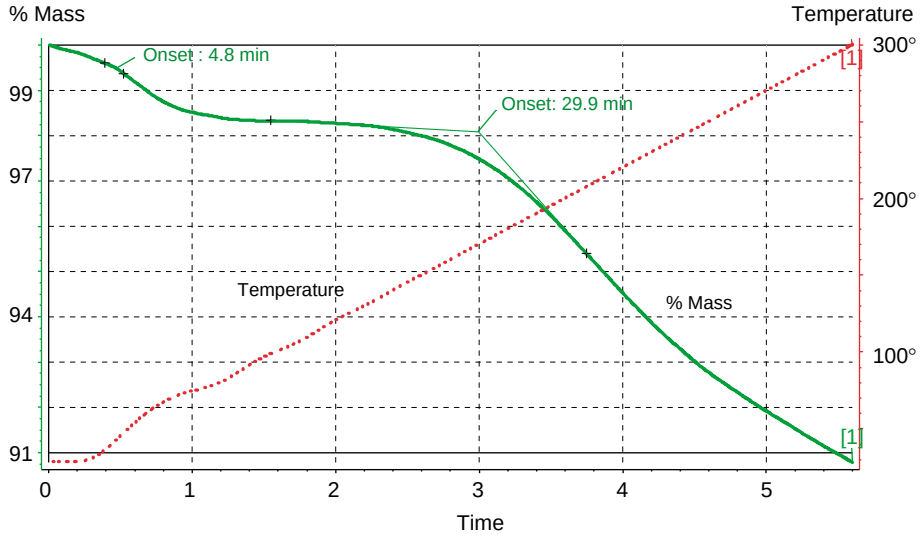


Fig. 3. TGA weight loss curve for 3:2 polyimide heated from 20 to 300 °C at 5 °C/min.

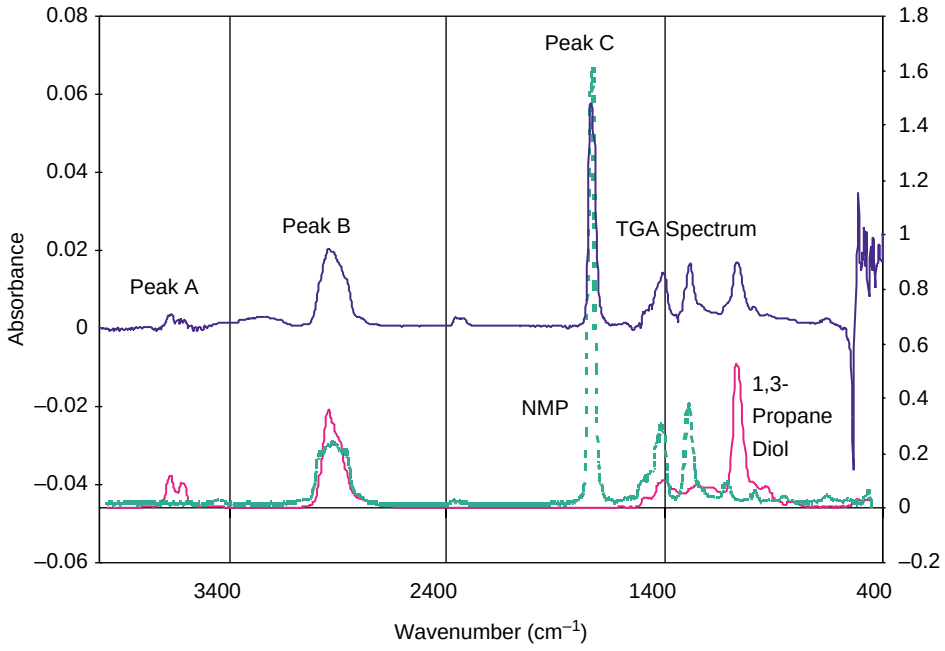


Fig. 4. IR spectra for 1,3-propane diol, NMP, and the evolved gases from TGA.

NMP peak at 1737 $cm^{-1}$ and the propane diol peak at 1067 $cm^{-1}$).

IR spectra are generally difficult to quantify due to varying absorptivities and concentrations between samples mandating the use of ratios to yield useful information. Fortunately, there are common and stand-alone peaks in both propane diol and NMP spectra. The peaks chosen for analysis are at about 3670, 2900, and 1740 $cm^{-1}$ corresponding to the O–H stretch, C–H stretch, and C=O stretch, respectively [17].

Each of these peaks in the three spectra shown in Fig. 4 was integrated using the IR software. The results are shown in Table 2.

The ratios of peaks A and C to peak B in the pure sample spectra are approximately equal to the ratios in any mixture of the two. Applying the ratios from the pure components to the independent A and C peaks from the experimental data gives the contribution of each component to the combined B peak. In this case, $B_{NMP}=1.34$, while $B_{PD}=0.83$, equating to a molar composition of 62% NMP. Converting to weight percents, the evolved gases consist of 32% propane diol and 68% NMP.

Although significant uncertainty exists whenever quantitative IR analysis is attempted, a check can be made on the values to determine if 32% propane diol is reasonable. Fig. 5 shows that approximately 7.5% of the fibers' weight was lost between 130 and 300 °C. If the ratio analysis is correct, 32% of the 7.5% total weight loss is attributable to propane diol, or 2.4% overall. The theoretical propane diol loss at 100% crosslinking is 2.6%. While this does not show conclusively that the method is valid, the fact that the data is not inconsistent (i.e. not greater than 100% crosslinking, for example) lends credence to the technique. This ratio method will thus be applied in the following sections, although with the awareness of considerable uncertainty.

### 3.3. TGA-IR analysis of crosslinking time dependence

Section 3.1 showed dissolution results that indicate little change in solvent resistance between 6 and 96 h of crosslinking. This result was tested further with TGA-IR. A polymer sample was heated to 110 °C for 1 h to remove residual water; the temperature was then raised to 200 °C and held for 24 h. The weight loss is plotted vs. time in Fig. 5.

The initial weight loss during the 110 °C step reflects removal of residual water that is followed by a relatively large weight loss (~5%) during heating to 200 °C. The IR spectrum at this point is identical to that shown in Fig. 4, showing the presence of both NMP and propane diol. After the initial heating, very little weight loss occurs over the subsequent 24 h, and the IR registers no evolved components indicating that the crosslinking reaction with its evolution of propane diol occurs very quickly during initial heating to 200 °C.

Table 2
Peak integrals at 3670, 2900 and 1740 $cm^{-1}$ for the three spectra shown in Fig. 4

| Peak label | Frequency ($cm^{-1}$) | Stretch | Peak area | | |
|---|---|---|---|---|---|
| | | | Propane diol | NMP | Experimental |
| A | 3670 | O–H | 8.62 | N/A | 0.19 |
| B | 2900 | C–H | 36.74 | 33.42 | 2.54 |
| C | 1740 | C=O | N/A | 55.15 | 2.21 |

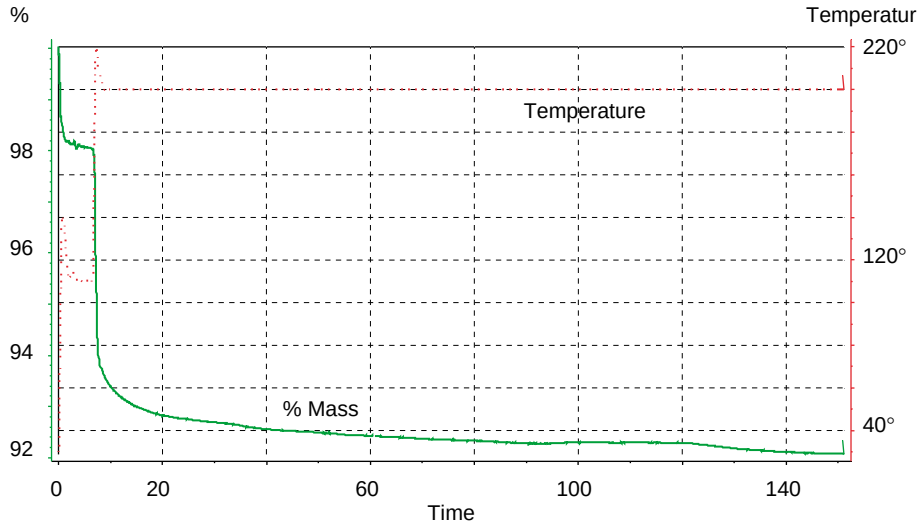


Fig. 5. TGA weight loss curve for 3:2 polyimide heated for 1 h at 110 °C and then held at 200 °C for 24 h.

Fig. 6 shows the 3D IR spectrum from a 3 h soak at 200 °C, and the lack of signal subsequent to the weight loss at about 80 min (4800 s) is evident. Except for the minor water signal at the beginning, the only absorbance is seen during heating to 200 °C, and it disappears thereafter.

Dissolution tests confirm that crosslinking occurred in samples treated for as little as 3 h, as they did not dissolve in THF. The fundamental crosslinking and loss of propane diol appears to be very rapid, occurring within 30 min of heating.

### 3.4. TGA-IR analysis of crosslinking temperature

In order to investigate the effect of temperature further, the TGA curve presented in Fig. 3 was analyzed and the weight loss onset identified at about 170 °C. The components evolved during the weight loss at 30 min were identified in Section 3.2 as propane diol and NMP. At temperatures below 170 °C in this ramp experiment, little propane diol is evolved, and thus limited crosslinking can be occurring, while at temperatures above 170 °C, propane diol is produced rapidly, evidence that crosslinking is happening.

To test this hypothesis, two runs were done, each with a 110 °C drying step for 1 h, followed by 3 h of treatment at either 150 or 180 °C (Fig. 7). It is immediately evident that less weight is lost in the 150 °C run than in the 180 °C trial. Information from the IR again shows that propane diol and NMP are both evolved during both runs. Integration of the peaks and applying the ratio technique discussed above shows that propane diol contributes 30% of the weight loss at 150 °C and 27% of the weight loss at 180 °C.

Table 3 summarizes the data from the two samples, as well as from a sample soaked for 3 h at 200 °C. The weight losses are taken only from the heating phase, as the subsequent slow weight loss does not show an IR signal, and can, therefore, not be conclusively identified.

By stoichiometry, 100% crosslinking would result in a 2.6% propane diol weight loss. According to the data in Table 3, 50% of this weight loss has occurred at 150 °C within 35 min (the window over which weight loss was measured), and the polymer remains soluble in THF while exhibiting an increased molecular weight (Section 3.1). At 180 °C, 69% of the weight loss has occurred, while at 200 °C, the loss has reached 73% of the theoretical maximum, and at both temperatures the polymer is insoluble in THF. Higher temperatures were not tested with this procedure, but from Section 3.2, a heat ramp to 300 °C results in 92% of total weight loss. These values are valid only within the uncertainty of the IR quantification, but a clear trend is seen. Increasing the temperature increases the amount of propane diol evolved, but as the theoretical maximum is approached, further temperature increases bring diminishing returns. The amount of propane diol evolved is certainly related to the degree of crosslinking, although a direct correlation would be difficult to justify.

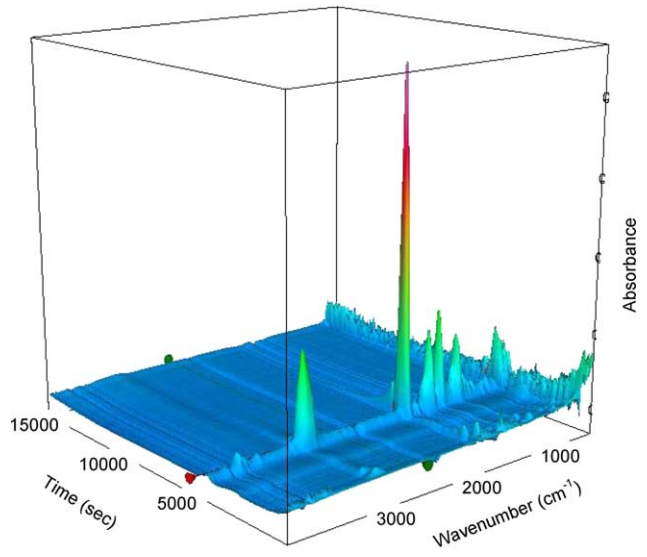


Fig. 6. Three-dimensional IR spectrum showing the evolution of components over 3 h during heating at 200 °C as in Fig. 8. The plot includes an initial 3600 s drying step at 110 °C. The large peaks occur at the point of heating from 110 to 200 °C.

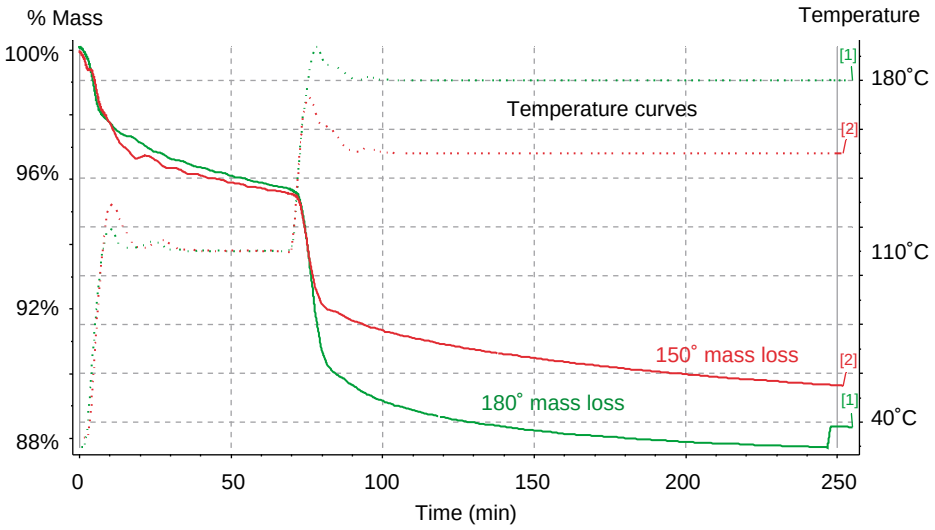


Fig. 7. TGA weight loss curve of 3:2 polyimide heated to 110 °C for 1 h, then held at 150 or 180 °C for 3 h.

Table 3
Estimated NMP and propane diol loss during heating of 3:2 polyimide to 150, 180 and 200 °C

| | 150 °C soak temperature | 180 °C soak temperature | 200 °C soak temperature |
|---|---|---|---|
| Percent weight loss during heating | 4.4 | 6.7 | 7.8 |
| Percent weight loss due to NMP | 3.1 | 4.9 | 5.9 |
| Percent weight loss due to propane diol | 1.3 | 1.8 | 1.9 |

### *3.5. Summary and analysis of TGA-IR data*

Three conclusions can be drawn from the TGA-IR data:

1. A significant amount of NMP remains in the fibers after drying (5–6%).
2. Crosslinking happens in as little as 30 min.
3. A minimum temperature (~180 °C) is required to cause significant crosslinking to occur.

These conclusions are consistent with a concept that balances temperature-induced chain mobility with chain immobilization caused by crosslinking. Esterification is an exothermic equilibrium reaction with high activation energy [18]. Activation energy barriers in chemical reactions are overcome by the thermally activated 'collisions' between reactants [19], while chain segment mobility enables bringing the reactive sites together. By removing the evolved 1,3-propane diol by vacuum or nitrogen purge, the equilibrium reaction can be forced to favor the crosslinked product. Thus, the desired crosslinking reaction would be expected to proceed to completion when exposed to a temperature high enough to provide adequate chain mobility, and a vacuum or inert sweep to remove propane diol.

The data obtained from TGA-IR experiments shows this not to be the case, indicating another factor at work. Instead of proceeding to completion, the reaction reaches a temperature-dependent equilibrium, presumably related to reduced mobility as crosslinking proceeds. In this case, 'equilibrium' is established, based not on chemical interactions, but on the mobility competition between elevated temperature and immobilizing crosslinks. The reaction is rapid at sufficient temperature, with the extent of reaction also set by that temperature.

### *3.6. Plasticization curves*

Another reflection of crosslinking is offered by the plasticization behavior of the fibers in the presence of aggressive agents like $CO_2$. A so-called 'plasticization pressure' can be defined as the minimum in a common 'U-shaped' permeation isotherm [20], although other isotherms have been identified, including the cases of no plasticization and 'immediate' plasticization [21]. 'Immediate' plasticization is commonly found in very thin films or asymmetric hollow fibers where no minimum is observed, but permeance remains relatively stable below the plasticization point, and begins to rise exponentially at higher pressures. Plasticization resistance is shown in more stability in the permeance at lower pressures, followed by a lesser response to higher $CO_2$ pressures.

Fig. 8 shows the permeation isotherm for three fiber states, one uncrosslinked and the other two crosslinked for 24 h at 120 and 200 °C, respectively. The uncrosslinked fiber shows an upswing in permeance almost immediately. The response is very large at higher pressures, with a permeance increase of 400% between 100 and 700 psi. Crosslinking shows an immediate reduction in this plasticization response. Some

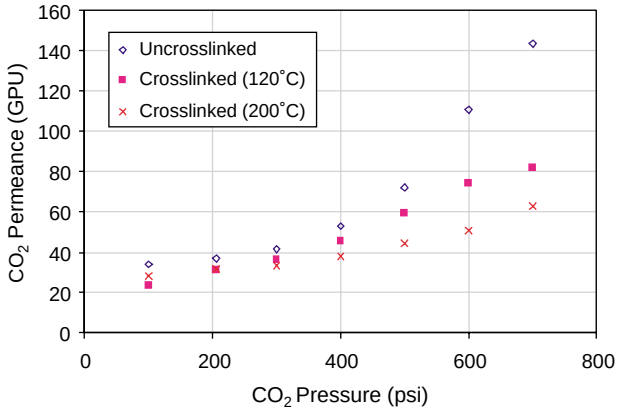


Fig. 8. Pure $CO_2$ permeance isotherm for uncrosslinked fibers and fibers crosslinked at 120 and 200 °C for 24 h. Test temperature = 30 °C. Uncertainty is ±5%.

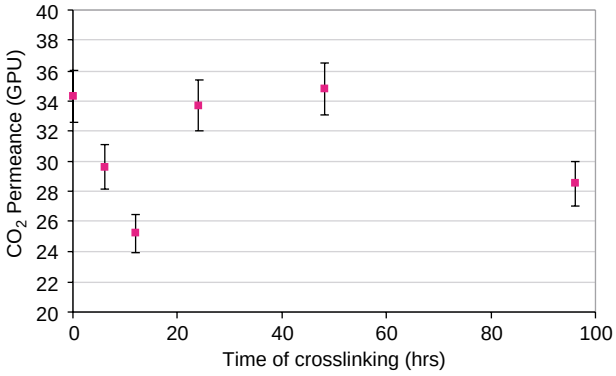


Fig. 9. Effect of crosslinking time on performance of fibers crosslinked at 200 °C for 6–96 h. Test conditions = 200 psi total feed pressure, 80/20 $CH_4/CO_2$ feed, 30 °C test temperature. Error bars are ±5%.

reduction in the plasticization response is seen for fibers treated at 120 °C, but the permeance still increases almost four-fold over the same pressure range. The fibers crosslinked at 200 °C showed the best plasticization resistance of the three, maintaining a relatively stable permeance up to about 350 psi before slowly rising somewhat. In the TGA-IR analysis, it was shown that the crosslinking reaction is more dependent on temperature than time. $CO_2$ permeation isotherms for fibers crosslinked between 6 and 96 h at 200 °C show similar results, as each curve has a similar reduction in plasticization response as compared to the uncrosslinked fibers.

The stability of crosslinked fibers is even more evident when compared to fibers spun from Matrimid®, a commercially available non-crosslinked polymer used for industrial gas separation membranes. Comparisons with Matrimid® fibers spun similarly to those described in this work show a productivity advantage at lower $CO_2$ pressures and significantly greater stability at 800 psi of pure $CO_2$.

## 4. Effects of crosslinking conditions on transport

Studies were undertaken to investigate the effect of crosslinking conditions on the transport properties of the fibers, as stability alone is insufficient for commercial application. Two pairs of gases were studied, $O_2/N_2$ and $CO_2/CH_4$. Oxygen and nitrogen were studied as pure gases, while a 20% $CO_2$ in $CH_4$ mixture was used as a model natural gas feed to test $CO_2/CH_4$ separation performance.

Both pairs of gases showed clear effects of crosslinking that were difficult to adequately describe. As the crosslinking temperature and time were increased, permeance and selectivity would rise and fall, indicating that subtle sorption and diffusion phenomena were occurring. Although chemical studies with TGA-IR and solubility indicated a strong temperature and weak time dependence on the amount of crosslinking, permeation measurements showed significant effects from both crosslinking time and temperature. Fig. 9 shows $CO_2$ permeance vs. crosslinking time as a representative trend.

Each of the other factors ($O_2$, $N_2$, $CH_4$ permeance and $O_2/N_2$, $CO_2/CH_4$ selectivity) showed similar effects of oscillating performance as the time or temperature of crosslinking was varied. This shows the complexity of the system as the various conditions result in different degrees of chemical crosslinking, solvent removal, and morphological changes to both skin and substructure layers. The more detailed discussion of these phenomena [14] shows that the addition of chemical crosslinking to complex asymmetric fiber structures requires significant attention to all details of processing.

## 5. Feed conditions and post-treatment

### 5.1. Effect of pressure on transport properties

Fiber performance at low pressures provides a convenient and useful benchmark for comparison. For many applications, however, fibers must perform under more demanding high-pressure conditions. The fibers tested here were crosslinked at 200 °C for 48 h and had a $CO_2/CH_4$ selectivity of about 32 and a $CO_2$ permeance of 35 GPU at 200 psi. The hollow fiber module was tested at a series of pressures between 200 and 1000 psi, and the $CO_2/CH_4$ selectivity dropped 16% over that pressure range. No hysteresis was observed; reducing the pressure back to 200 psi regained essentially all of the original selectivity.

The drop in selectivity can be explained by the competing sorption effects of the two gases. Since, the difference in fugacity between carbon dioxide and methane are already accounted for in the calculations, the differences in the pressure responses reflects competition between the two components for existing unrelaxed volume as described by the dual mode theory of sorption [22]. In the absence of plasticization (shown by the lack of hysteresis), the sorption coefficient tends to decrease with increasing pressure as Langmuir sorption sites are filled, and this reduced sorption coefficient leads to lower permeance. Since, $CO_2$ sorbs more strongly than $CH_4$, its permeance is more affected, resulting in a decrease in $CO_2/CH_4$ selectivity.

### 5.2. Effect of high pressure on transport properties

For industrial applications, it is important not only that performance be maintained as pressure is increased, but the performance must be stable over time at high pressures. In order to begin to simulate long-term exposure to a high $CO_2$ content natural gas stream, the fibers discussed in Section 5.1 were exposed to a 20% $CO_2$ in $CH_4$ feed at 1000 psi of total pressure for approximately 100 h. Over the course of these 4 days, the $CO_2/CH_4$ selectivity remained near 28, while the permeance stabilized at about 27 GPU after initial creep over the first 24 h.

Although 4 days represents only the initial phase of stability testing, the critical observation here is that plasticization, with its accompanying selectivity loss, does not occur over this time period. Even more important than the stability at 1000 psi was the lack of hysteresis seen on depressurization. When these fibers were tested again at 200 psi, the original permeance and selectivity were regained, indicating a lack of plasticization. Longer testing periods are still needed to establish stability over weeks and months, but these initial tests indicate good stability.

### 5.3. Effect of skin layer caulking

Although these fibers show good stability in the face of $CO_2$, the $CO_2/CH_4$ selectivity still falls short of current commercial membranes. Industrially, 'caulking' is often used to repair nanoscopic defects in the selective layer, and thereby raise the selectivity of hollow fibers [23]. The fibers used in this work were caulked with silicone rubber using a standard procedure [24] to investigate the possibility of raising the selectivity, and an immediate improvement was apparent. At 200 psi total feed pressure, $CO_2/CH_4$ selectivity increased by nearly 50% from 30 to 44 indicating that the initial fibers skins were slightly defective, although those defects could be caulked with common techniques.

While the fiber performance improved significantly at low pressures, Fig. 10 shows the advantage to be short-lived. As the pressure was raised from 200 to 1000 psi, the $CO_2/CH_4$ selectivity dropped steadily, and continued to do so when held at 1000 psi. Unlike the uncaulked fibers, a significant hysteresis effect was observed, and the original selectivity was never regained. Given the prevalence of the caulking technique in industry, it is important to understand that the stability of the base polymer is only part of the issue; fibers must be spun with high intrinsic selectivity from the start, or the stability of the caulking layer must be addressed as well.

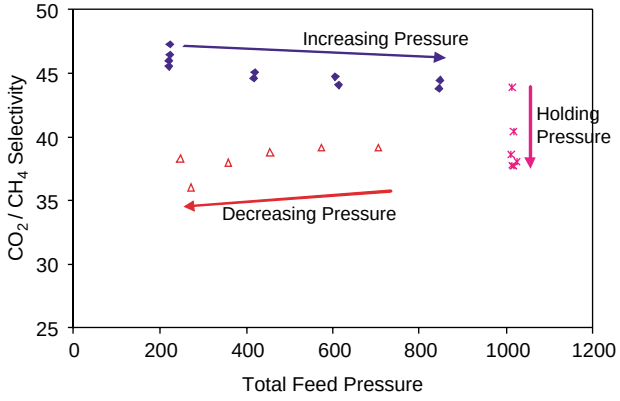


Fig. 10. Effect of feed pressure on $CO_2/CH_4$ selectivity of caulked fibers originally crosslinked for 48 h at 200 °C. 80/20 $CH_4/CO_2$ feed, 30° test temperature. Uncertainty is ±7%.

### 5.4. Effect of temperature on transport properties

Industrial application of these membranes may require operation at temperatures above 30 °C, so the performance of the fibers at 50 °C was chosen as a model operating temperature. The post-treated crosslinked fibers described in Section 5.3 were tested with an 80% $CH_4$, 20% $CO_2$ feed at 200 psi at this feed temperature.

The silicone post-treated fibers exhibited a 33% loss in selectivity from 30 to 50 °C. At the lower temperatures, $CO_2/CH_4$ selectivity was 43, while at 50 °C, selectivity dropped to 30. This is approximately the same selectivity that is found for uncaulked, crosslinked fibers at 30 °C. Further investigation is required to determine if the selectivity loss would be significantly reduced in fibers that do not require post-treatment.

## 6. Covalent crosslinking with catalyst

### 6.1. Catalyst background

Section 3 demonstrated that the crosslinking of these fibers is a complex interaction of mobility and reactivity. By lowering the activation energy for reaction through the use of a catalyst, and by slightly plasticizing the matrix with a low swelling diluent to increase segmental mobility, the limitation to reaction may be able to be reduced sufficiently to enable higher crosslinking degree at a given temperature, or the temperature to achieve a specified degree of crosslinking could be reduced.

Esterification reactions are acid-catalyzed [18], and thus the addition of an acid catalyst could lower the activation energy needed to drive the reaction forward. *para*-Toluenesulfonic acid (PTSA) has been shown to be useful in catalyzing polyesterification reactions [25], and is used to catalyze the monoesterification of the polymers used in this work. The application of catalyst can also be extended to the *trans*-esterification step by impregnating a membrane with the acid prior to heat treatment. A 0.6 M PTSA solution in ethanol was used during the solvent exchange process to imbibe the catalyst into the fibers. Subsequent washing with hexane and drying trapped the catalyst in the polymer matrix. Sulfur analysis indicated 4% (wt) residual PTSA in the fibers after drying.

Fibers were then crosslinked under vacuum for 24 h at 120, 150, and 180 °C. All three sets of fibers were insoluble in THF, indicating that the catalyst was effective in encouraging the crosslinking reaction. Table 4, however, shows that the transport properties of the ideal gas pair $O_2/N_2$ were negatively

Table 4
Ideal gas performance of unpost-treated fibers, before and after crosslinking with the aid of the PTSA catalyst

| Catalyst/crosslinking | $O_2$ permeance (GPU) | $N_2$ permeance (GPU) | $O_2/N_2$ selectivity |
|---|---|---|---|
| As-spun fiber, no catalyst, uncrosslinked | 5.4 | 1.2 | 4.5 |
| Fiber with catalyst, uncrosslinked | 1.3 | 0.7 | 1.9 |
| Fiber with catalyst crosslinked at 120 °C | 1.6 | 1.0 | 1.6 |
| Fiber with catalyst crosslinked at 150 °C | 1.0 | 0.5 | 2.0 |
| Fiber with catalyst crosslinked at 180 °C | 1.5 | 0.6 | 2.5 |

Testing was done with pure gases at 30 °C and 100 psi feed pressure. Uncertainty is ±5% for permeance values, and ±7% for selectivity.

affected. Similar to the complex effects of crosslinking time and temperature on transport properties discussed above, the use of catalyst has repercussions beyond encouraging the crosslinking reaction at lower temperatures. As it is expected that lower temperatures are advantageous for commercial application, further investigation with other promising catalysts, such as methylsufonic acid [26,27], or even non-acid (less polar) catalysts like titanium butoxide [28] should be undertaken. Alternatively, a catalyst such as oxalic acid could be used that would degrade during the crosslinking process, thus minimizing its effect on the final fibers.

## 7. Conclusions

Asymmetric hollow fibers were spun from crosslinkable polyimides. The fibers showed nearly defect-free selectivity for $O_2/N_2$ separations. Crosslinking was carried out under a range of temperatures and exposure times. Varying the crosslinking conditions caused slight changes in $O_2/N_2$ separation performance, primarily due to changes in the morphology of the fibers (densification of transition and skin layers).

The crosslinking was characterized by dissolution studies, TGA-IR analysis, and plasticization tests. These studies revealed that the crosslinking reaction is rapid, occurring within 30 min of exposure to sufficient temperature. The minimum temperature to cause noticeable solvent resistance in the absence of catalyst was found with TGA to be around 170 °C. Dissolution studies showed that higher temperatures resulted in less swelling, indicating slightly higher crosslink density. These data support a picture of the reaction as limited primarily by an activation energy that must be overcome by chain mobility in order to drive the crosslinking reaction forward.

The crosslinked fibers showed improvement in plasticization resistance as compared to uncrosslinked fibers. Higher crosslinking temperatures improved resistance, while longer crosslinking times appeared to have a limited effect on plasticization resistance.

Fiber separation performance was found to be highly dependent on the conditions of crosslinking, both time and temperature. The rapid nature of crosslinking appears to be valid only for initial solvent and plasticization resistance, while $CO_2/CH_4$ permeance and selectivity show more subtle effects. Substructure collapse seems to be occurring in treatment at all temperatures and times, offset by improvements in material properties at some temperatures. The maximum performance was found at a crosslinking condition of 200 °C for 48 h, with a selectivity of 32 and a $CO_2$ permeance of 35 GPU (measured using 80/20 mol% $CH_4/CO_2$ feeds at 200 psi feed pressure and 30 °C).

Some loss in performance was seen as pressure was increased, and crosslinked fibers also showed stability at high pressures, maintaining selectivity and permeance over the course of 4 days exposure to 1000 psi. Post-treatment of the crosslinked fibers raised their selectivity to over 40, although at higher pressures, the advantage of post-treatment was lessened. Higher temperature testing of the post-treated fibers also showed significant performance decline, although the post-treated fibers still had higher selectivity than their untreated counterparts under identical testing conditions.

Catalysts were employed to reduce the temperature required for crosslinking. Dissolution studies showed that fibers treated at temperatures as low as 120 °C were resistant to dissolution in THF. The separation performance of catalyst-crosslinked fibers was greatly diminished due to the method of catalyst impregnation and further optimization is needed in this area.

## Acknowledgements

The authors are grateful for financial support from the ChevronTexaco Energy Research and Technology Corporation and the Department of Energy Basic Energy Sciences under grant DE-FG02-04ER15510.

## References

[1] Bos A, Punt IGM, Wessling M, Strathmann H. Sep Purif Technol 1998; 14:27–39.
[2] Bos A, Punt IGM, Wessling M, Strathmann H. J Polym Sci, Part B: Polym Phys 1998;36:1547–56.
[3] Bos A, Punt IGM, Strathmann H, Wessling M. AIChE J 2001;47: 1088–93.
[4] Kita H, Inada T, Tanaka K, Okamoto K. J Membr Sci 1994;87(1–2): 139–47.
[5] Liu Y, Wang R, Chung TS. J Membr Sci 2001;189(2):231–9.
[6] Fang J, Kita H, Okamoto K. J Membr Sci 2001;182:245–56.
[7] Staudt-Bickel C, Koros WJ. J Membr Sci 1999;155(1):145–54.
[8] Wind JD, Staudt-Bickel C, Paul DR, Koros WJ. Macromolecules 2003; 36(6):1882–8.
[9] Wind JD, Staudt-Bickel C, Paul DR, Koros WJ. Ind Eng Chem Res 2002; 41(24):6139–48.
[10] Koros WJ, Fleming GK. J Membr Sci 1993;83:1–80.
[11] Krol JJ, Boerrigter M, Koops GH. J Membr Sci 2001;184(2):275–86.
[12] Wallace D, Staudt-Bickel C, Koros W. J Membr Sci 2005; in press.
[13] McKelvey SA, Clausi DT, Koros WJ. J Membr Sci 1997;124(2):223–32.
[14] Wallace D. PhD Dissertation, University of Texas, Austin; 2004.
[15] Kesting RE, Fritzsche AK. Polymeric gas separation membranes. New York: Wiley; 1993.
[16] NIST Mass Spec Data Center, S.E. Stein, director, "Infrared Spectra" in NIST Chemistry WebBook, NIST Standard Reference Database Number

69, Eds. P.J. Linstrom and W.G. Mallard, June 2005, National Institute of Standards and Technology, Gaithersburg MD, 20899 (http://webbook.nist.gov).
[17] Lambert JB, Shurvell HF, Lightner DA, Cooks RG. Organic structural spectroscopy. Upper Saddle River, NJ: Prentice Hall; 1998.
[18] Bruice PY. Organic chemistry. Englewood Cliffs, NJ: Prentice Hall; 1995.
[19] Moore WJ. Physical chemistry. 3rd ed. Englewood Cliffs, NJ: Prentice-Hall Inc.; 1962.
[20] Koros WJ, Hellums MW. Transport properties. Encyclopedia of polymer science and engineering; 1990. p. 724–802.
[21] Bos A. PhD Dissertation, University of Twente; 1996.
[22] Michaels AS, Vieth WR, Barrie JA. J Appl Phys 1963;14(1):13–20.
[23] Murphy MK, Beaver ER, Rice AW. AIChE Symp Ser 1989; 85(272):34–40.
[24] Carruthers SB. PhD Dissertation, University of Texas, Austin, TX; 2001.
[25] Kuo CT, Chen S. J Polym Sci, Part A: Polym Chem 1989;27(8): 2793–803.
[26] Schmerling L. Primary alkyl esters, USA 3474131.
[27] Putzig DE, McBride EF, Do HQ, Trainham JA, Jaeger HL, Schulte H. Compositions and process of titanium-containing catalysts for esterification or transesterification and polycondensation, USA 6255441.
[28] Lindall CM, Ridland J, Slack N. Organometallic esterification catalysts and process for preparation of an ester, WO 2003045550.